A multiscale model for piezomagnetic behavior

Karl-Joseph Rizzo, Olivier Hubert, Laurent Daniel

A multiscale model for piezomagnetic behavior - Coupled anhysteretic multiscale and hysteretic Jiles-Atherton approaches

Karl-Joseph Rizzo[a,b], Olivier Hubert[a], Laurent Daniel[b]

[a] *LMT-Cachan (ENS Cachan/CNRS UMR 8535/UPMC/UniverSud Paris) 61, avenue du Président Wilson - 94235 CACHAN Cedex - France*
[b] *LGEP (SUPELEC, CNRS(UMR 8507), UPMC, Univ Paris Sud) 11, rue Joliot-Curie - Plateau du Moulon - 91192 Gif sur Yvette Cedex - France*

Abstract

This work is concerning the development of a stress sensor for high strain rate applications (Hopkinson bar apparatus). The physical principle of the sensor is based on the piezomagnetic behavior of remanent magnetic material. Experiments consist in anhysteretic and hysteretic piezomagnetic measurements of a low carbon steel. We then propose a model for the piezomagnetic behavior based on a modified formulation of Jiles model and a multi-scale model for the anhysteretic part. Modeling and experiments are in good agreement.

Keywords:
piezomagnetic behavior, dynamic sensor, multiscale modeling, Jiles model

1. Introduction

The Hopkinson bar apparatus is the usual tool to identify the mechanical behavior of materials at high strain rates [7]. The impact is provided by a projectile (striker) launched at high velocity V_0 against an incident bar (input bar), which crushes the specimen against the transmitted bar (output bar - see Figure 1). The measurements (stress $\sigma(t)$, celerity) are generally provided by strain gauges cemented on the bars [14]. Figure 2 shows an example of compressive stress wave during an impact with Hopkinson bar apparatus. This measurement is carried out by strain gauges.

The use of a pick-up coil wound around a previously magnetized Hopkinson bar (remanent or submitted to a constant magnetic field H) is an alternative possible solution (Figure 1). When passing through the coil, the stress wave produces

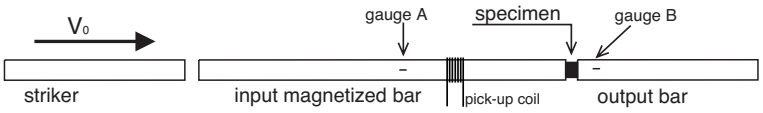

Figure 1: Hopkinson bar apparatus with pick-up coil wound on a magnetized bar

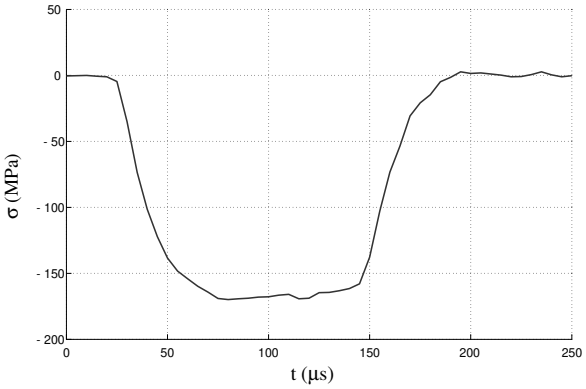

Figure 2: Measurement of the stress level during an impact using Hopkison bar apparatus - strain gauges measurement

an *emf* signal $V(t)$ (Figure 3a). This signal is the expression of a change in magnetization M following Lenz law [1] (see Figure 3b) where B, n and S denote respectively the magnetic induction, the number of turns of the coil and its area (μ_0 is the permeability of air).

$$V(t) = nS\frac{dB}{dt} = nS\mu_0\frac{dM}{dt} = nS\mu_0\frac{dM}{d\sigma}\frac{d\sigma}{dt} \tag{1}$$

$$\sigma(t) = \frac{1}{nS\mu_0}\int\left(\frac{dM(H=Cst,\sigma)}{d\sigma}\right)^{-1}V(t)dt \tag{2}$$

The change of magnetization due to stress $M(\sigma)$ is corresponding to the piezomagnetic behavior of the material [5]. $M(\sigma)$ is usually non-linear, non-monotonous and hysteretic [13, 8]. The stress $\sigma(t)$ can then be theoretically estimated from the *emf* signal $V(t)$ using a time integration procedure [2]. Such an estimation supposes to precisely know the derivative expression $dM/d\sigma$ at constant field and so require a mathematical modeling of $M(\sigma)$ function including its hysteretic character.

Experimental results have been discussed extensively elsewhere [11, 8]. The main results presented herein illustrate the different mechanisms involved in the

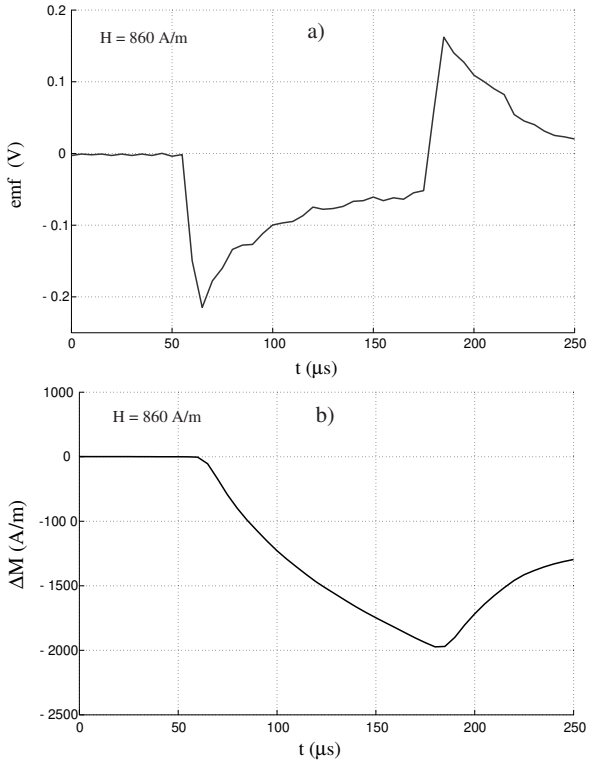

Figure 3: Impact provided by Hopkinson bar apparatus: a) measurement of the emf signal; b) associated variation of magnetization - the magnetic field level is estimated at H = 860 A/m

phenomenon and the influence of some parameters (amplitude, frequency, magnetic field level). In this study, we focused on modeling aspects of the anhysteretic and hysteretic piezomagnetic behavior. We especially use a so-called multiscale model in order to compute the anhysteretic piezomagnetic behavior [4]. This model naturally takes both stress and magnetic field loading into account. The modeling of the piezomagnetic hysteresis is made thanks to a modified formulation of Jiles-Atherton hysteretic model for ferromagnetic behavior [10].

2. Experimental procedure

The material used for the experiments is a low carbon steel (0.2wt% C), for which the behavior[1] is very close to the behavior of a pure iron. A first step was

[1]Mechanical, magnetic and magneto-mechanical (magnetostrictive) behaviors.

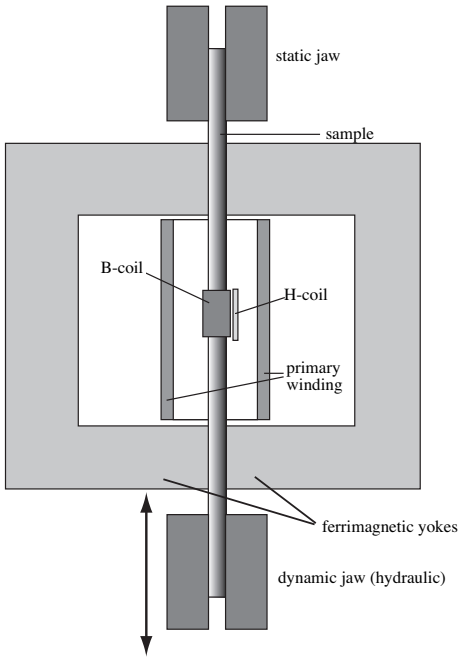

Figure 4: Experimental set-up

to get the reversible piezomagnetic behavior from anhysteretic magnetic measurements carried out under static uniaxial stress (from -180 MPa to +180 MPa). Figure 4 shows the experimental set-up that has been used and the experimental procedure is explained in [11]. A sinusoidal stress waveform has been used for the dynamic piezomagnetic measurements. Parameters are the mean stress $\bar{\sigma}$ (-180 MPa to +180 MPa), the stress amplitude $\Delta\sigma$ (0 MPa to 180 MPa), the frequency f (5 Hz to 50 Hz) and the static magnetic field level H (0 A/m to 10000 A/m). The procedure is composed of following steps: 1-demagnetization; 2- application of the mean stress $\bar{\sigma}$; 3-application of the static magnetic field (anhysteretic procedure is applied); 4- cyclic mechanical loading of amplitude $\Delta\sigma$; 5- averaging over 100 cycles; 6- numerical integration of the *emf*; 7- evaluation of the integration constant by comparisons to the anhysteretic behavior (the anhysteretic point is kept as a reference point).

3. Experimental results and discussion

Anhysteretic $M(H,\sigma = Cte)$ measurements lead to conventional results for a low carbon steel: strongly non-linear magnetization curve; strong decrease of

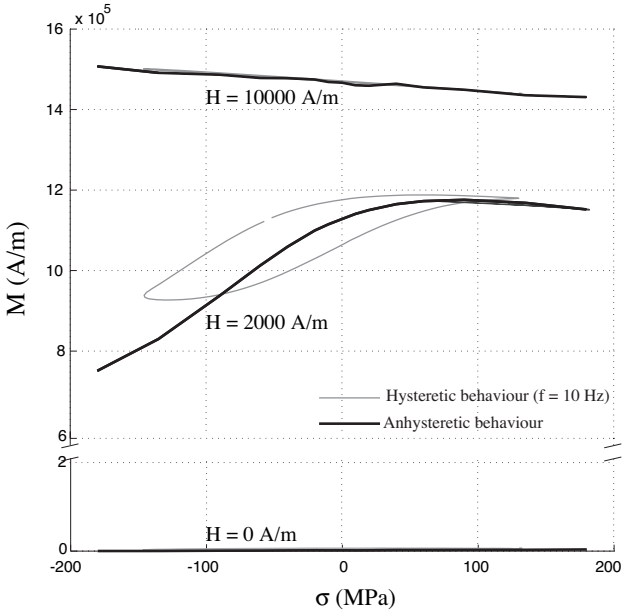

Figure 5: Anhysteretic and hysteretic piezomagnetic behavior of the material for three different magnetic field levels (H = 0 A/m; H = 2000 A/m; H = 10000 A/m); f = 10 Hz

susceptibility due to compressive stress, weak improvement due to tensile stress and so-called Villari reversal at intermediate fields. Thick black lines in Figure 5 give a piezomagnetic representation of these results ($M(\sigma, H = Cte)$). At zero magnetic field, magnetization stays zero whatever stress level and sign. This point is in accordance with the fact that stress has a quadratic influence on domain distribution. In a weak to intermediate magnetic field, $dM/d\sigma$ ratio is roughly positive (positive magnetostriction). It reaches its highest value for $H \approx$ 1000 A/m and a low compressive level ($\sigma \approx$-10 MPa). The Villari reversal is associated with a change of $dM/d\sigma$ sign. This mechanism occurs for a more or less high stress level depending on the magnetic field strength [8].

It denotes the beginning of a magnetization rotation due to stress. High magnetic fields ($\geq$ 8 kA/m) lead to a negative linear variation of $M(\sigma)$ (with $dM/d\sigma \approx -$ 250 A/m/MPa).

Figure 5 shows on the other hand the typical cyclic magnetic responses associated with the variation of stress ($\bar{\sigma}$ = -10 MPa, $\Delta\sigma$ = 140 MPa, f = 10 Hz) for zero applied field, H = 2000 A/m and H = 10000 A/m (Gray lines). The piezomagnetic hysteresis betrays the existence of dissipative phenomena associated to two usual mechanisms: the macroscopic and/or microscopic Eddy currents that brake

the displacement of the domain wall (dynamic losses), and the pinning-unpinning mechanism (hysteretic losses). This is in accordance with the progressive disappearance of cycle at high magnetic field.

On the other hand, the piezomagnetic cycles are not symmetric: positive stress leads to a quasi-reversible situation; negative stress does apparently increase the dissipation; This result is clearly confirmed by the measurements plotted in Figures 6a, 6b and 6c. Increasing amplitudes always lead to an increase of dissipation. Compression experiments are always more dissipative than tensile experiments.

Let consider an iron single crystal initially separated in 6 domain families, associated to the 6 easy directions, in equal proportion. Figure 7 illustrates the dissymmetry of change of the domain structure when the single crystal is submitted to a traction or a compression. Iron is a positive magnetostriction material; a traction is progressively simplifying the domain structure so that the quantity of domain walls is decreasing. In this simplified example, only 180^o domain walls subsist. Because a varying stress does not move a 180^o domain wall, it does not lead to any dissipation. The domain structure associated with a negative stress is more complicated. Density of domain walls stays high and their displacements lead to a much higher dissipation.

4. Multiscale modeling of the anhysteretic piezomagnetic behavior

Multiscale approaches are of great interest when the phenomena are the result of anisotropies at different scales [1]. Three scales are considered: polycrystal, single crystal and magnetic domain scales.

4.1. Microscopic modeling

The microscopic model of magneto-elastic behavior of single crystals proposed first by [1] was recently modified to avoid any minimization procedure [3]. A grain is seen as an assembly of magnetic domains. A magnetic domain α is defined by its magnetization vector $\vec{M}_\alpha$ [3] (M_s is the saturation magnetization of the material; γ_i are the direction cosines of the magnetization) and its magnetostriction tensor ε_α^μ [4] (λ_{100} et λ_{111} are the magnetostrictive constants of the single crystal). The potential energy [5] of a magnetic domain is corresponding to the sum of the magneto-crystalline [6], magnetostatic [7] and magneto-elastic [8] energies. Because the magnetization is supposed homogeneous within each domain, and domain walls contribution is neglected, the exchange energy is not considered [4]. Moreover uniform strain and magnetic field hypotheses have been used for the calculations.

$$\vec{M}_\alpha = {M_s}^t(\gamma_1;\gamma_2;\gamma_3) \tag{3}$$

$$\varepsilon^\mu_\alpha = \frac{3}{2}\begin{pmatrix} \lambda_{100}(\gamma_1^2-\frac{1}{3}) & \lambda_{111}\gamma_1\gamma_2 & \lambda_{111}\gamma_1\gamma_3 \\ \lambda_{111}\gamma_1\gamma_2 & \lambda_{100}(\gamma_2^2-\frac{1}{3}) & \lambda_{111}\gamma_2\gamma_3 \\ \lambda_{111}\gamma_1\gamma_3 & \lambda_{111}\gamma_2\gamma_3 & \lambda_{100}(\gamma_3^2-\frac{1}{3}) \end{pmatrix} \tag{4}$$

$$W_\alpha = W_\alpha^H + W_\alpha^\sigma + W_\alpha^K \tag{5}$$

$$W_\alpha^K = K_1(\gamma_1^2\gamma_2^2+\gamma_2^2\gamma_3^2+\gamma_3^2\gamma_1^2) + K_2(\gamma_1^2\gamma_2^2\gamma_3^2) \tag{6}$$

$$W_\alpha^H = -\mu_0\overrightarrow{M}_\alpha.\overrightarrow{H}_\alpha \approx -\mu_0\overrightarrow{M}_\alpha.\overrightarrow{H}_g \tag{7}$$

$$W_\alpha^\sigma = \frac{1}{2}(\sigma_\alpha : \mathbb{C}_g^{-1} : \sigma_\alpha) \approx -\sigma_g : \varepsilon_\alpha^\mu \tag{8}$$

$\overrightarrow{H}_\alpha$, σ_α, $\overrightarrow{H}_g$ and σ_g respectively correspond to the magnetic field and stress in a domain α and in a grain g. $\mathbb{C}_g$ is the stiffness tensor of the single crystal, K_1 and K_2 are the anisotropy constants of the material. The volumetric fraction f_α of each domain α is seen as the probability of existence of this domain comparing to the others. It is expressed thanks to a Boltzmann function written as function of the potential energy of the domains :

$$f_\alpha = \frac{\exp(-A_s.W_\alpha)}{\int_\alpha \exp(-A_s.W_\alpha)d\alpha} \tag{9}$$

f_α is function of the unique adjustable parameter A_s. This parameter can be easily deduced from low field experimental magnetization curve. It is shown in [4] that $A_s = 3\chi_0/(\mu_0.M_s^2)$, where χ_0 is the initial anhysteretic susceptibility of the material. Assuming that the elastic behavior is homogeneous within a grain, the magnetostriction strain of a single crystal is written as the mean magnetostriction of each domain [10] ($< .. >$ denotes an averaging operation). The magnetization in a grain is defined as well [11].

$$\varepsilon_g^\mu = <\varepsilon_\alpha^\mu> = \int_\alpha f_\alpha\,\varepsilon_\alpha^\mu d\alpha \tag{10}$$

$$\vec{M}_g = <\vec{M}_\alpha> = \int_\alpha f_\alpha\,\vec{M}_\alpha d\alpha \tag{11}$$

This procedure does not require any minimization process since any orientation is supposed to be considered and its probability of existence correctly defined. It requires nevertheless a large number of orientations to minimize numerical approximations. For this work, 10242 domain orientations regularly distributed in the space have been used for each grain. The main advantage of this formulation is that it does not require any preliminar definition of easy magnetization direction and associated domain family. As a consequence the numerical difficulties associated to the instability of some domain families submitted to a stress disappear.

4.2. Localization and homogenization

A polycrystalline ferromagnetic media can be considered as an aggregate of single crystals assembled following the orientation data. The microscopic level modeling is applied for each grain of the polycrystalline aggregate. The magnetization at polycrystalline scale is defined as the average value of magnetization at grain scale [12]. A local demagnetizing field in each grain due to the magnetization of the surrounding grains is introduced [4]: the magnetic field at the grain scale $\vec{H}_g$ is defined as a function of the external field $\vec{H}$, the mean secant equivalent susceptibility of the material χ_m, ($\chi_m = M/H$) and the difference between the mean magnetization $\vec{M}$ and the magnetization at the grain scale $\vec{M}_g$ [13]. The elastic behavior is obtained thanks to a self-consistent homogenization scheme. The macroscopic magnetostriction strain [14] is estimated using the Eshelby's solution and considering the local magnetostriction as a free strain; $\mathbb{B}$ denotes the fourth order stress concentration tensor [6].

$$\vec{M} = < \vec{M}_g > \tag{12}$$

$$\vec{H}_g = \vec{H} + \frac{1}{3 + 2\chi_m}(\vec{M} - \vec{M}_g) \tag{13}$$

The magnetostriction strain at grain scale is elastically incompatible and creates a stress that have to be added to the applied stress. The stress at grain scale σ_g is so derived from the implicit Equation [15].

$$\varepsilon_\mu = < {}^t\mathbb{B} : \varepsilon_g^\mu > \tag{14}$$

$$\sigma_g = \mathbb{B} : \sigma + \mathbb{C}^{acc} : (\varepsilon^\mu - \varepsilon_g^\mu) \tag{15}$$

with $\mathbb{C}^{acc} = ((\mathbb{C}_g)^{-1} + (\mathbb{C}_0 : ((\mathbb{S}^{Esh})^{-1} - \mathbb{I}))^{-1})^{-1}$. $\mathbb{C}_0$ is the stiffness tensor of

the effective media [6]. As a self-consistent scheme has been chosen, $\mathbb{C}_0$ refers to the self-consistent stiffness tensor. σ is the macroscopic applied stress. $\mathbb{S}^{Esh}$ is the so-called Eshelby's tensor. Since this model always refers to equilibrium, modeling results are anhysteretic.

In this work, the orientation data file for the definition of the polycrystalline media is issued from a regular spheric mapping of the space (546 orientations). The mechanical and magnetic characteristics of iron are used for the calculations. The modeling has been implemented in the same loading conditions than the experimental ones: constant applied magnetic field H ($\vec{H} = H.\vec{z}$) and uniaxial macroscopic stress σ ($\sigma = {}^t\vec{z}.\sigma.\vec{z}$) defined by its mean value and amplitude. Figure 8 shows the results of anhysteretic piezomagnetic simulations $M(\sigma)$ ($\vec{M} = M.\vec{z}$) for various magnetic field levels (from 0 A/m to 10000 A/m) and $\sigma \in$[-180;+180] MPa. Since this calculation is anhysteretic, the mechanical loading path has no importance. Results are qualitatively coherent with experimental results (especially the slope at saturation). Parameters used for the calcultation are listed in Table 1.

Table 1: Physical constants used for the multiscale modeling

coefficient	M_s	K_1 ; K_2	λ_{100} ; λ_{111}	A_s	C_{11} ; C_{12} ; C_{44}
unit	A/m	kJ.m^{-3}	10^{-6}	m^3.J^{-1}	GPa
value	1.71x10^6	42.7; 15	21 ; -21	2x10^{-2}	238 ; 142 ; 232

5. Jiles-Atherton modeling of the piezomagnetic hysteresis

The anhysteretic behavior $M(\sigma)$ is given by the multiscale modeling. This expression must be enriched by a hysteretic component. We propose to model the hysteretic part of the piezomagnetic behavior thanks to a formulation derived from Jiles-Atherton modeling of magnetic hysteresis [10].

5.1. Jiles-Atherton modeling of the magnetic hysteresis

The model initialy proposed by Jiles *et al*. (1984) is a scalar modeling of the magnetic hysteresis $M(H)$. It uses on the one hand the anhysteretic magnetic behavior which is corresponding to the behavior of the ideal material and is written:

$$M_{an} = M_s(cotan(H_e/a) - a/H_e) \tag{16}$$

with

$$H_e = H + \beta.M \tag{17}$$

H_e is the effective magnetic field function of the applied field H and of the anhysteretic magnetization[2]. β is a localization factor. In Equation [16], a is a parameter associated to the initial slope of the anhysteretic curve.

Moreover, Jiles considered the magnetization M as the sum of a reversible and an irreversible part. The reversible magnetization is linked to the movement of domain walls close to their equilibrium position. The irreversible magnetization is linked to the jumps of domain walls from one pinning site to another. The hysteretic part of the model is driven by a differential equation defining the rate of irreversible magnetization as a function of the gap between the ideal magnetization (anhysteretic) and the actual magnetization (irreversible). After a few calculations, one gets the following relation between M, M_{an} and H without applied stress.

$$\frac{dM}{dH} = \frac{(1-c).(M_{an}-M)}{(1-c).k\delta - \beta.(M_{an}-M)} + c.\frac{dM_{an}}{dH} \tag{18}$$

c is a constant associated to the reversible bending of the domain walls. δ is a directionnal parameter equal to 1 or -1 depending on the sign of dH/dt. k is the damping factor strongly correlated to the quantity of dissipated energy.

5.2. Extension of the Jiles-Atherton model to the piezomagnetic hysteresis

Piezomagnetism means variation of magnetization due to a variation of stress. The variation of magnetization dM can then be defined as the sum of two *a priori* uncoupled contributions: contribution of magnetic field on the one hand and contribution of stress on the other hand [19]. dM/dH is corresponding to the classical Jiles-Atherton differential equation (see paragraph above). $dM/d\sigma$ is the piezomagnetic term. Expressing the effect of stress on the magnetization at constant magnetic field is possible using the multiscale modeling. It gives the anhysteretic part of the behavior. Concerning the dissipative mechanisms, we observe that a stress can act on the magnetic microstructure very similarly comparing to a magnetic field. Bending of domain walls or pinning/un-pinning are mechanisms that could occur. The driving force is now the magnetoelastic energy term. A simple re-writting of the Jiles-Atherton model leads to the expression [20].

[2]When a stress is considered, H_e can be written as function of stress too [12].

$$dM = \frac{dM}{dH}.dH + \frac{dM}{d\sigma}.d\sigma \tag{19}$$

$$\frac{dM}{d\sigma} = \frac{(1-c_\sigma).(M_{an}-M)}{(1-c_\sigma).k_\sigma\delta - \beta_\sigma.(M_{an}-M)} + c_\sigma.\frac{dM_{an}}{d\sigma} \tag{20}$$

c_σ is a constant associated to the reversible bending of the domain walls due to stress. δ is a directionnal parameter equal to 1 or -1 depending on the sign of $d\sigma/dt$. k_σ is the damping factor correlated to the quantity of dissipated energy. Parameters c_σ and k_σ are a priori different from c and k considering the fact that stress mainly acts on 90^o domain walls, and magnetic field on 180^o domain walls. Another point is that we have to take into account that the domain structure change is different for a traction or a compression (Figure 7). As already discussed, the difference of domain wall quantity observed for a same amplitude in traction or compression explains the dissymetry in the experimental results. This mechanism is associated to the parameter k_σ which has to be different in traction and compression. We decided to use the following relation for k_σ:

$$k_\sigma = k_0 + k_a.\sigma \text{ for } \sigma < 0 \text{ and } k_\sigma = k_0 \text{ for } \sigma > 0 \tag{21}$$

Parameter β_σ is more difficult to interpret: it is associated to the effect of magnetization on stress heterogeneity (stress localization). We decided to consider this parameter as zero neglecting the strain incompatibilities. Figure 9 shows an example of calculation of the piezomagnetic hysteresis. Parameters used for the calculation are indicated in Table 2. This Figure shows on the other hand the effect of parameter k_a. Uniform stress and field hypotheses have been used for the calculation of the anhysteretic behavior.

Finally Figures 10a and 10b show respectively the influence of the level of applied magnetic field and the influence of the amplitude of stress on the piezomagnetic response. Results are in good agreement with the experimental observations. However, the modeling overestimates the magnetization at low and medium magnetic field. The assumption of uniform stress and field partly explains this disagreement because it neglects the effect of elastic incompatibilities and demagnetizing fields. The current model can take these phenomena into account but becomes much more costly in terms of computational time. On the other hand, the model does only represent the hysteretic losses. The width of cycles is therefore lower than the experimental cycles. Figure 11 shows for example the experimental piezomagnetic behavior for different frequencies. 10 Hz frequency clearly leads

to dynamic losses: the cycle at 10 Hz is different from the cycle at 5 Hz. Low frequency signal are nevertheless difficult to measure.

Table 2: Parameters used for piezomagnetic hysteresis modeling

Parameters	c_σ	k_0	k_a	β_σ
unit	-	Pa	-	Pa.m.A^{-1}
value	0.8	16x10^6	0.2	0

6. Conclusion

The construction of a sensor based on a so highly non-linear, non-monotonic and hysteretic behavior such as the piezomagnetic behavior requires an accurate modeling. The modeling presented herein is a first step. It will be improved by the introduction of the effect of frequency to reflect the dynamic losses. This work is in progress on the basis of Jiles model extended to the dynamic behavior [9]. The long term objective is however to overcome the limitations of a phenomenological model such as Jiles model. The central idea is to introduce in the multiscale modeling a dissipative term based on the description of the physical mechanisms responsible for the dissipation. For example, the calculation of the rate of volumetric fraction could provide indicators of dissipation linked to the movement of domain walls [2].

Bibliography

[1] N. Buiron, L. Hirsinger, and R. Billardon. Influence of the texture of soft magnetic materials on their magneto-elastic behaviour. *J. Phys. IV*, 11:373, 2001.

[2] N.A. Buznikov, A.S. Antonov, C.G. Kim, C.O. Kim, A.A. Rakhmanov, and S.S. Yoon. The effect of domain-walls motion on second harmonic amplitude of magnetoinductive response in co-based amorphous wires. *J. Magn. Magn. Mat.*, 285:314, 2005.

[3] L. Daniel and N. Galopin. A constitutive law for magnetostrictive materials and its application to terfenol-d single and polycrystals. *EPJ Appl. Phys.*, 42:153, 2008.

[4] L. Daniel, O. Hubert, N. Buiron, and R. Billardon. Reversible magneto-elastic behavior: A multiscale approach. *J. of the Mech. Phys. Sol.*, 56:1018, 2008.

[5] A.C. Eringen and G.A. Maugin. *Electrodynamics of Continua*. Springer Verlag, 1990.

[6] R. Hill. Continuum micro-mechanics of elastoplastic polycrystals. *J. of the Mech. Phys. Solids*, 13:213, 1965.

[7] Bob Hopkinson. A method of measuring the pressure in the deformation of high explosive by impact of bullet. *Trans. Royal Soc. of London*, 213:437, 1914.

[8] O. Hubert and K.J.: Rizzo. Anhysteretic and dynamic piezomagnetic behavior of a low carbon steel. *J. Magn. Magn. Mat.*, 320:979, 2008.

[9] D.C. Jiles. Modelling the effects of eddy current losses on frequency dependent hysteresis in electrically conducting media. *IEEE Transactions on Magnetics*, 30:4326, 1994.

[10] D.C. Jiles and D.L. Atherton. Theory of ferromagnetic hysteresis. *J. of Applied Physics*, 55:2115, 1984.

[11] L. Lollioz, S. Pattofatto, and O. Hubert. Application of piezo-magnetism for the measurement of stress during an impact. *J. of Elect. Engineering*, 57:10, 2006.

[12] M.J. Sablik, H. Kwun, G.L. Burkhardt, and D.C. Jiles. Model for the effect of tensile and compressive stress on ferromagnetic hysteresis. *J. of Appl. Phys.*, 61:3799, 1987.

[13] L. Vandenbossche, L. Dupré, and J. Melkebeek. Evaluating material degradation by the inspection of minor loop magnetic behavior using the moving preisach formalism. *J. of Applied Physics*, 99:08D907, 2006.

[14] H. Zhao. Material behaviour characterisation using shpb techniques, tests and simulations. *Computers & Structures*, 81(12):1301, 2003.

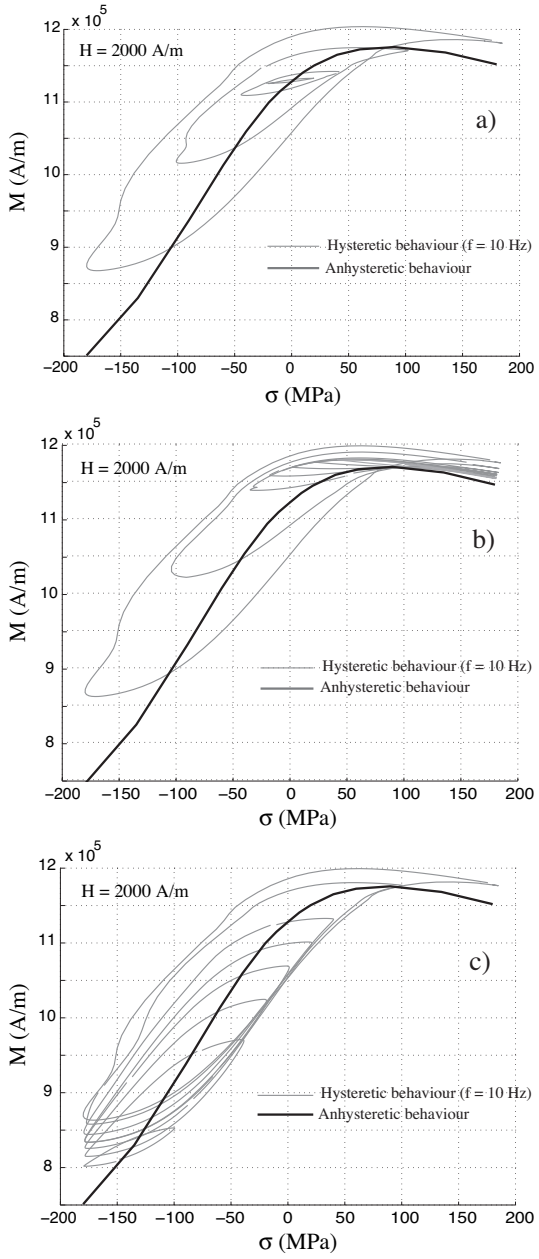

Figure 6: Hysteretic piezomagnetic behavior under cyclic stress conditions (H = 2000 A/m, f = 10 Hz)

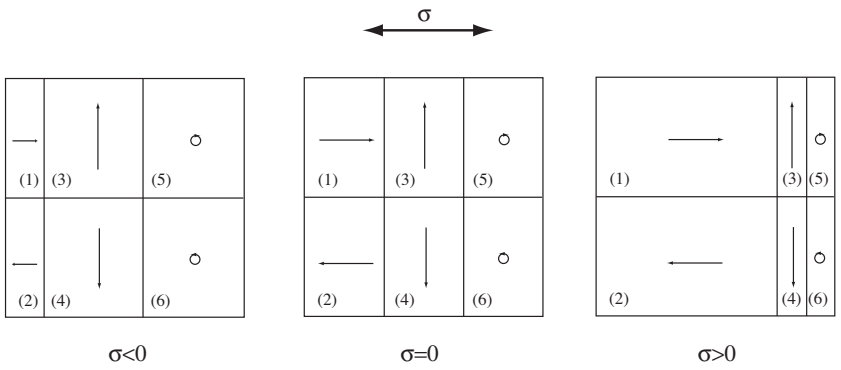

Figure 7: Illustration of the dissymmetry of change of the domain structure submitted to traction or compression - positive magnetostrictive material

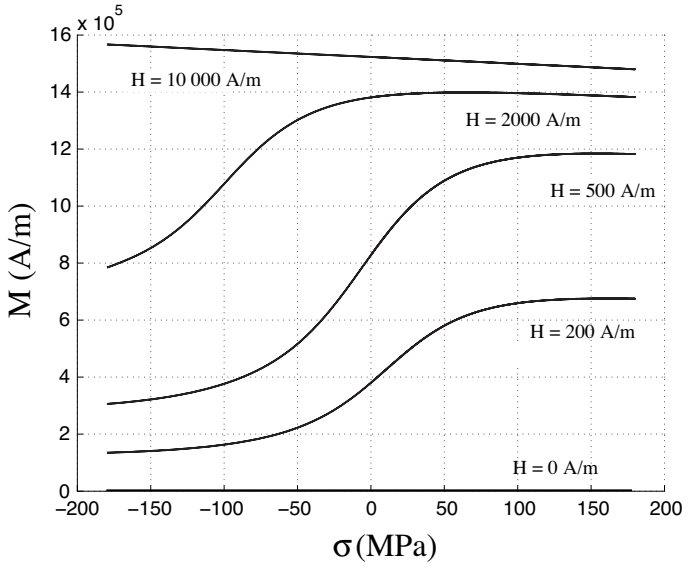

Figure 8: Results of the multiscale modeling for the anhysteretic piezomagnetic behavior - effect of the level of magnetic field

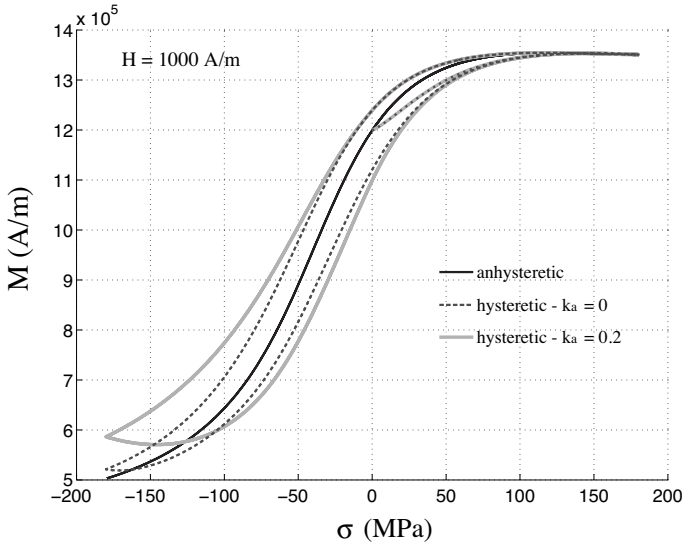

Figure 9: Results of the Jiles-Atherton modeling for the piezomagnetic behavior - change of the parameter between traction and compression

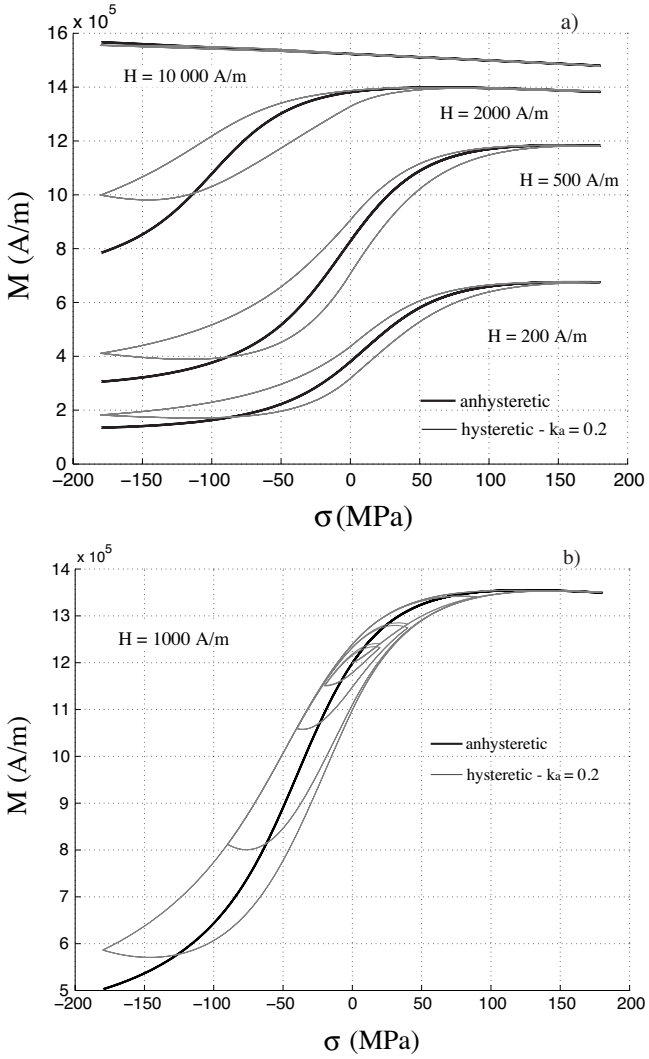

Figure 10: Results of the Jiles-Atherton modeling for the piezomagnetic behavior - effect of the level of magnetic field a) and stress amplitude b)

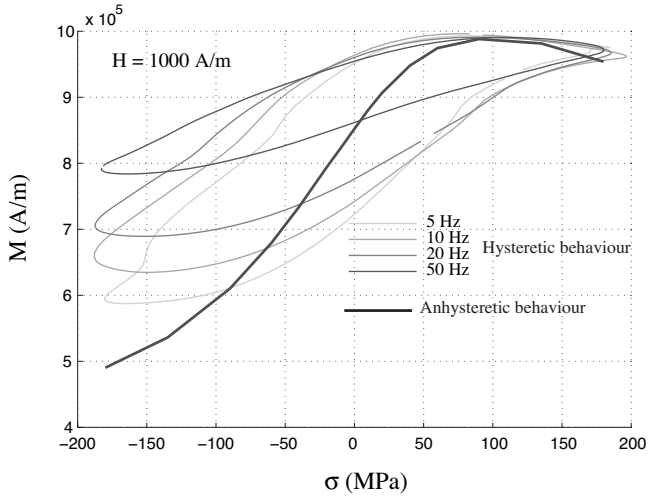

Figure 11: Experimental results of the effect of stress frequency on piezomagnetic hysteretic behavior; H = 1000 A/m